Supplementary Materials: Amazon Forests' Response to Droughts: A Perspective from the MAIAC Product. *Remote Sens*. 2016, *8*, 356.

Jian Bi, Ranga Myneni, Alexei Lyapustin, Yujie Wang, Taejin Park, Chen Chi, Kai Yan and Yuri Knyazikhin

1. Introduction

The supplementary section contains the detailed description of the data used, pre-processing of the data, and methods for calculating standardized anomalies of greenness and precipitation. Also included are supplementary figures from Figures S1–S9.

2. Data

2.1. Land cover

The land cover types over Amazon were identified using the MODIS land cover product MCD12Q1 [1]. MCD12Q1 provides land cover classes at 500 m for multiple classification systems, one of which is the International Geosphere Biosphere Program (IGBP) classification system. We aggregated the IGBP classes into 5 classes: forests, savannas, other vegetation, non-vegetation, and water (Figure S1). Forests include all the forest types: Evergreen Needleleaf forest, Evergreen Broadleaf forest, Deciduous Needleleaf forests, and Mixed forest; savannas include Woody savannas and Savannas; other-vegetation class includes all the remaining vegetated classes; non-vegetation class include: Urban and built-up, Snow and ice, and Barren or sparsely vegetated. The aggregated forest class indicates the distribution of Amazon forests.

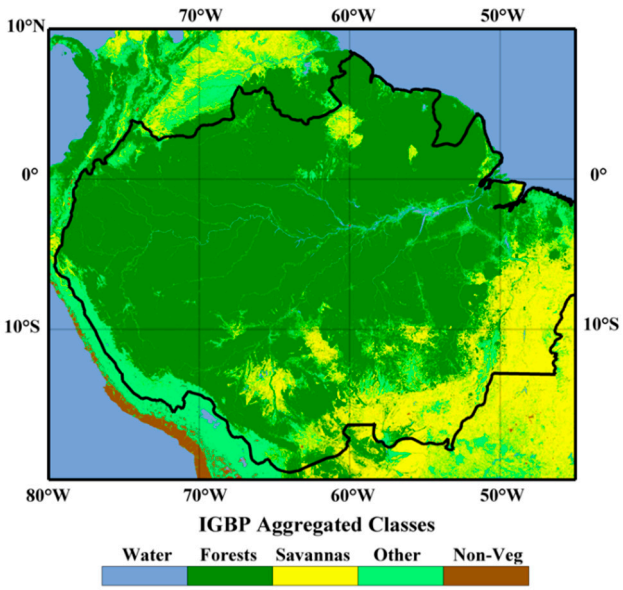

Figure S1. Land cover types over Amazon. The land cover types were identified using the IGBP classification system in the MODIS land cover product MCD12Q1.

2.2. Precipitation

We used the TRMM Product 3B43 (V7) to analyze the precipitation dynamics over Amazon. The 3B43 algorithm merges the TRMM satellite data and the Global Precipitation Climatology Center (GPCC) rain gauge analysis data to provide monthly estimates of precipitation from 1998 onward, at quarter degree spatial resolution for the area between 50°N and 50°S [2]. We used the TRMM 3B43

(V7) precipitation product from 2000 to 2012 to identify the drought regions over Amazonia in 2005 and 2010.

2.3. Collection 5 and Collection 6 MODIS Vegetation Index

The standard MODIS products currently provided by NASA include two versions: Collection 5 (C5) and Collection 6 (C6). The C6 products are the improved version of the C5 products, and one of the improvements in the C6 products is the updated sensor calibration. We call both the C5 and C6 versions the standard MODIS products.

The standard MODIS vegetation index products, MOD13A2 from Terra MODIS and MYD13A2 from Aqua MODIS, provide Normalized Difference Vegetation Index (NDVI) and Enhanced Vegetation Index (EVI) at 1 km spatial resolution and 16-day temporal frequency [3]. The retrieval algorithm picks the best observation to represent the vegetation photosynthetic activity during the 16-day period. The vegetation indices in standard MODIS VI products are from various sun-view geometries, and have Quality Assurance (QA) fields to indicate the quality of the retrieved vegetation index. These QA fields indicate the general quality of the retrieved vegetation index, the aerosol quantity, and the cloud and cloud shadow contamination status. The standard MODIS vegetation index products from both Terra and Aqua platforms during 2000 to 2012 were used in this study.

2.4. MAIAC Vegetation Index

The Multi-Angle Implementation of Atmospheric Correction (MAIAC) vegetation index (including NDVI and EVI) products are produced at 1 km spatial resolution and 8-day frequency using the MAIAC surface reflectance products. The MAIAC surface reflectance is retrieved from MODIS observations (with improved sensor calibrations with regard to Collection 5) using the MAIAC algorithm based on an accurate semi-analytical solution of the Ross-Thick Li-Sparse model [4–7]. The MAIAC algorithm also normalizes the retrieved surface reflectance to fixed sun-sensor geometry—45° solar zenith angle and nadir view—to exclude sun-sensor geometry variation and to make the remote observations on different dates comparable.

The MAIAC VI products provide valid vegetation indices only. Pixels with atmospheric contamination, including clouds and cloud shadows, do not have MAIAC vegetation index retrievals. The MAIAC cloud detection algorithm is more accurate and less conservative than the MODIS standard cloud detection algorithm, because it is based on time series and spatial analysis. MAIAC product obtains 20%~80% more cloud-free observations over tropical forests than standard MODIS product, depending on season [8]. MAIAC vegetation index products from both Terra and Aqua platforms during 2000 to 2012 were used in this study.

3. Methods

3.1. Filtering the Standard MODIS Vegetation Index Product

The standard MODIS vegetation index product contains Quality Assurance (QA) fields to indicate the quality of the provided vegetation index value. Some vegetation index values are contaminated by clouds or aerosols, and need to be screened out in our study. The filtering method used in our study is the same as in [9,10]. The retrieved MODIS vegetation index data were considered valid when (a) "MODLAND_QA" equals 0 or 1; (b) "VI Usefulness" is less than 11; (c) "Adjacent clouds detected" equals 0; (d) "Mixed clouds" equals 0; (e) "Possible shadows" equals 0; and (f) "Aerosol Quantity" equals 1 or 2. After this filtering using the QA information, there is still some residual atmospheric contamination in the standard MODIS VI data, so an additional filtering was applied as in [10]. The VI values that were two standard deviations or more away from the long term mean were filtered out to further exclude the atmospherically contaminated VI values from our study.

3.2. Standardized Anomaly

For each Amazon pixel, there were 13 dry-season mean values for precipitation (from 2000 to 2012), and at most 13 dry-season mean values for greenness (from 2000 to 2012 with possible missing values). We calculated the long-term mean and standard deviation using these available dry season mean values, and then calculated the standardized anomaly as the difference between the dry-season mean and the long-term mean, divided by the standard deviation. If either nominator or denominator did not exist, the standardized anomaly was tagged unavailable.

The spatial patterns of dry-season mean precipitation standardized anomalies from 2000 to 2012 over Amazon were illustrated in Figure S2, and the corresponding time series of the area of Amazonian forests with dry season precipitation standardized anomaly less than −1 were illustrated in Figure S3. The 2005 drought impacted mostly the western part of the Amazon basin, and the 2010 drought impacted a much larger area than the 2005 drought.

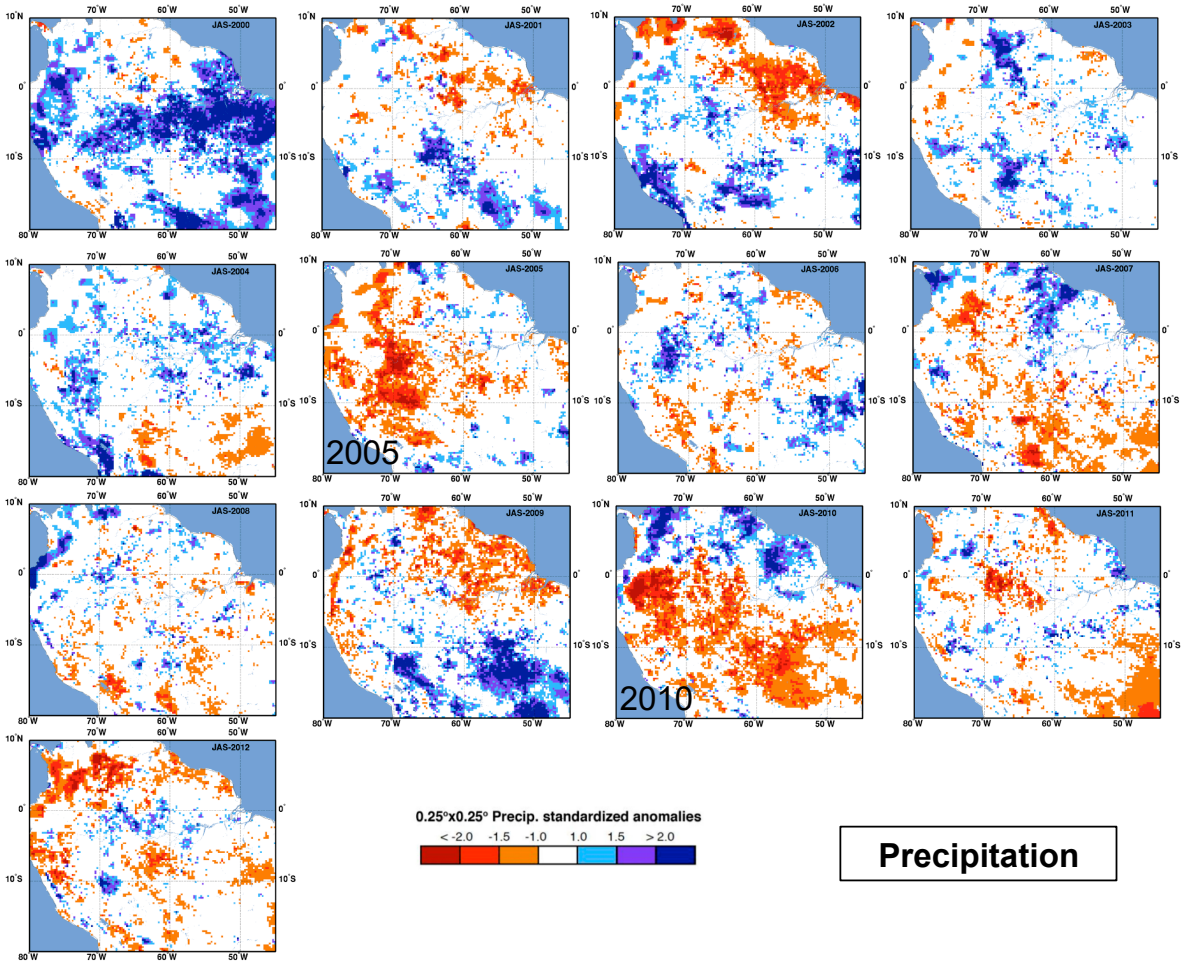

Figure S2. Spatial patterns of standardized anomalies of dry-season precipitation over Amazon in the years from 2000 to 2012. The TRMM precipitation data were used to identify the dry season precipitation anomalies.

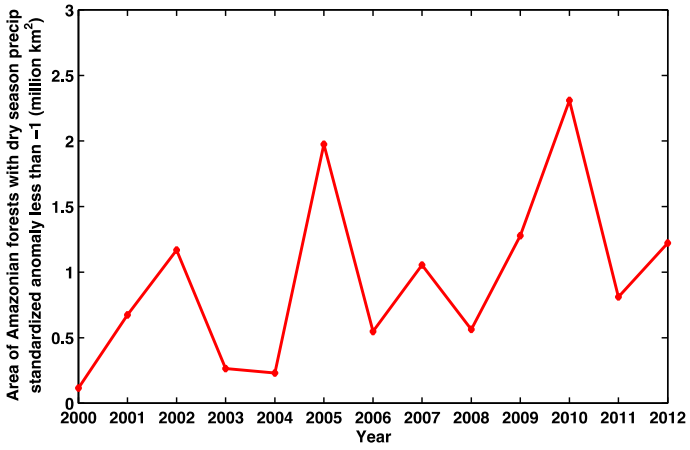

Figure S3. Area of Amazonian forests with dry season precipitation standardized anomaly less than −1 in the years from 2000 to 2012.

The dry-season mean greenness standardized anomalies from 2000 to 2012 were illustrated in Figures S4–S9. In 2000 and 2001, because we just had Terra data (Aqua was not launched untill 2002), the pixel availability was lower in these two years than in the other years.

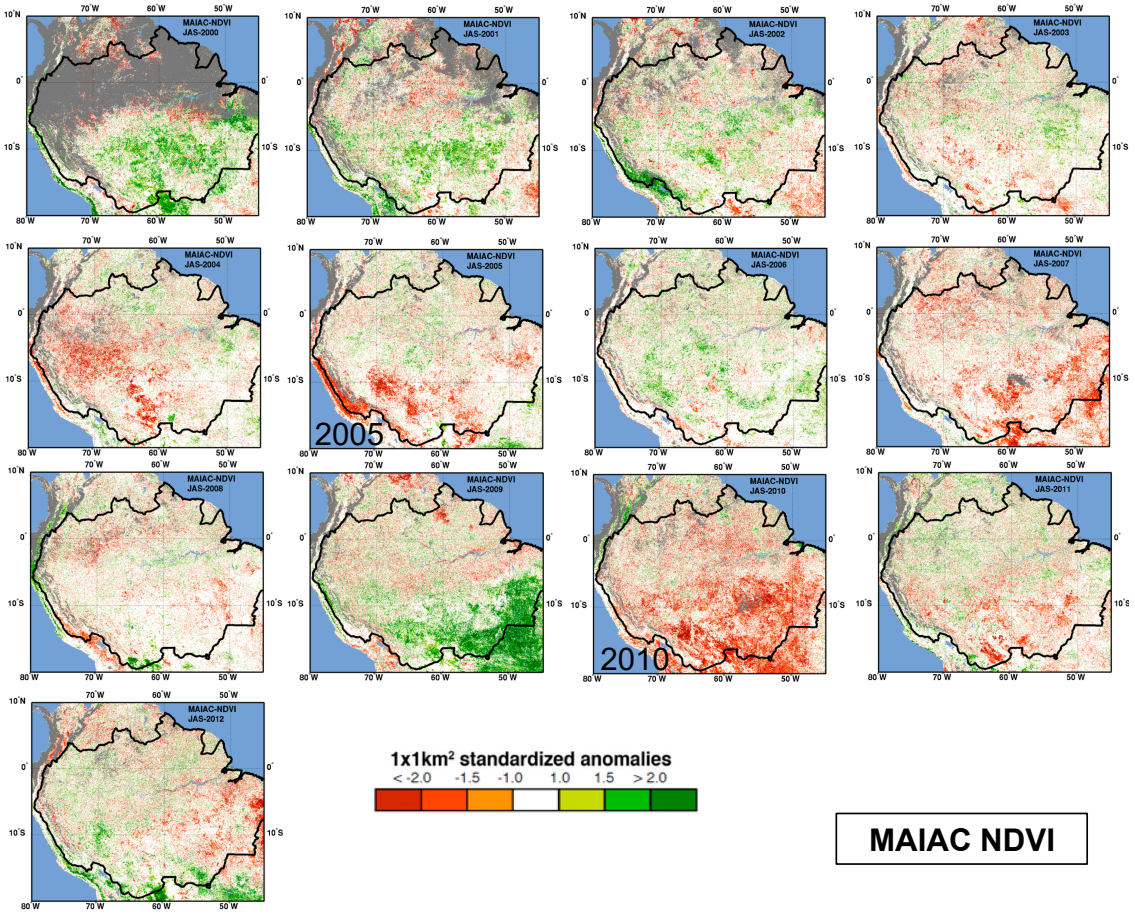

Figure S4. Spatial patterns of standardized anomalies of dry-season MAIAC NDVI over Amazon in the years from 2000 to 2012. Gray shaded areas are areas with missing data.

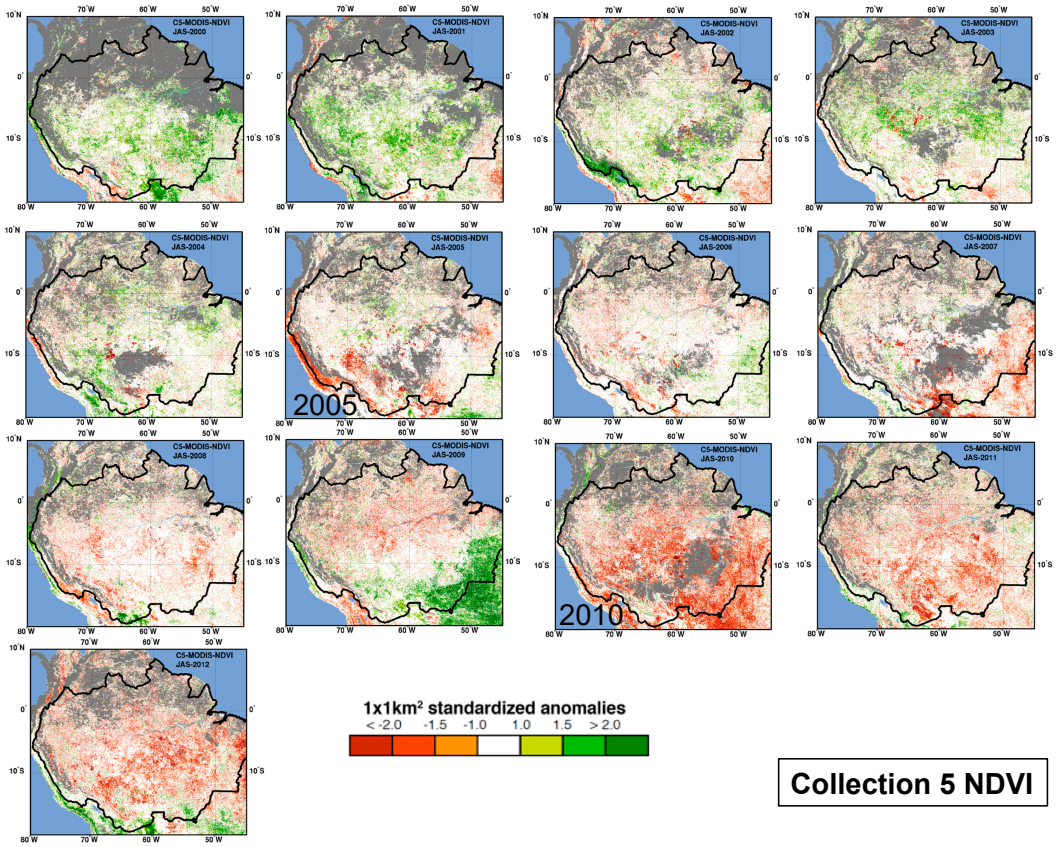

Figure S5. Spatial patterns of standardized anomalies of dry-season Collection 5 NDVI over Amazon in the years from 2000 to 2012. Gray shaded areas are areas with missing data.

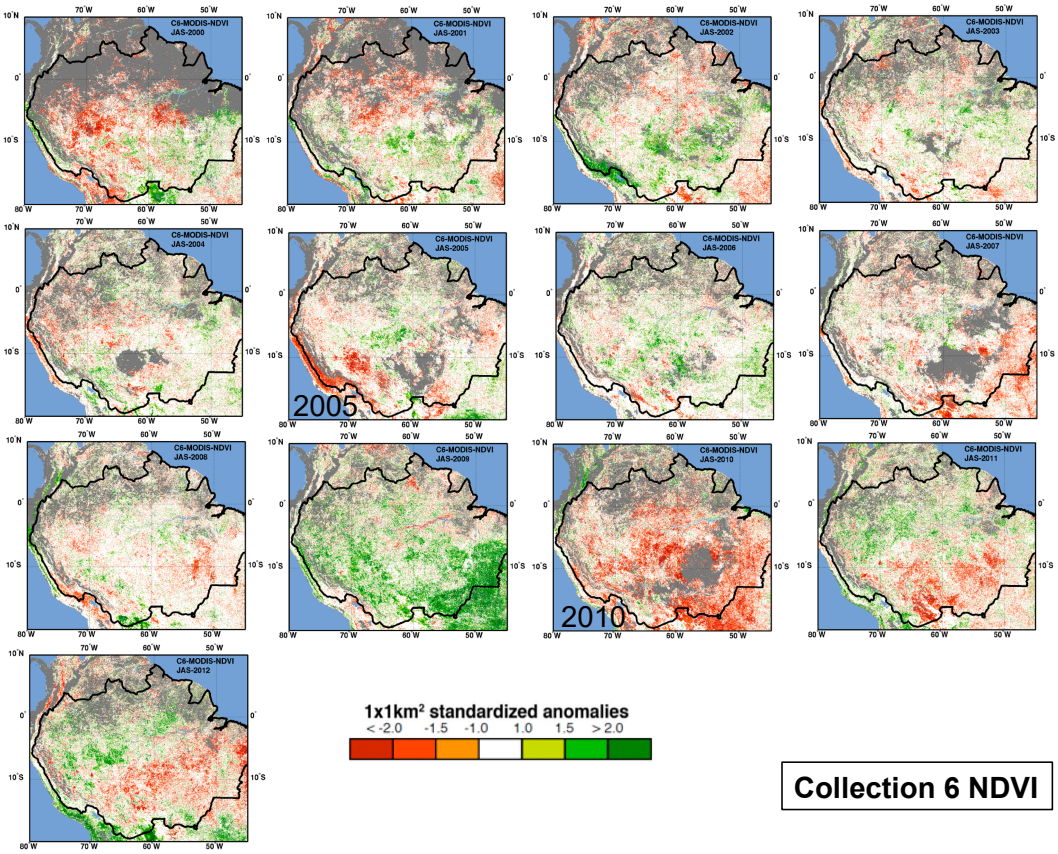

Figure S6. Spatial patterns of standardized anomalies of dry-season Collection 6 NDVI over Amazon in the years from 2000 to 2012. Gray shaded areas are areas with missing data.

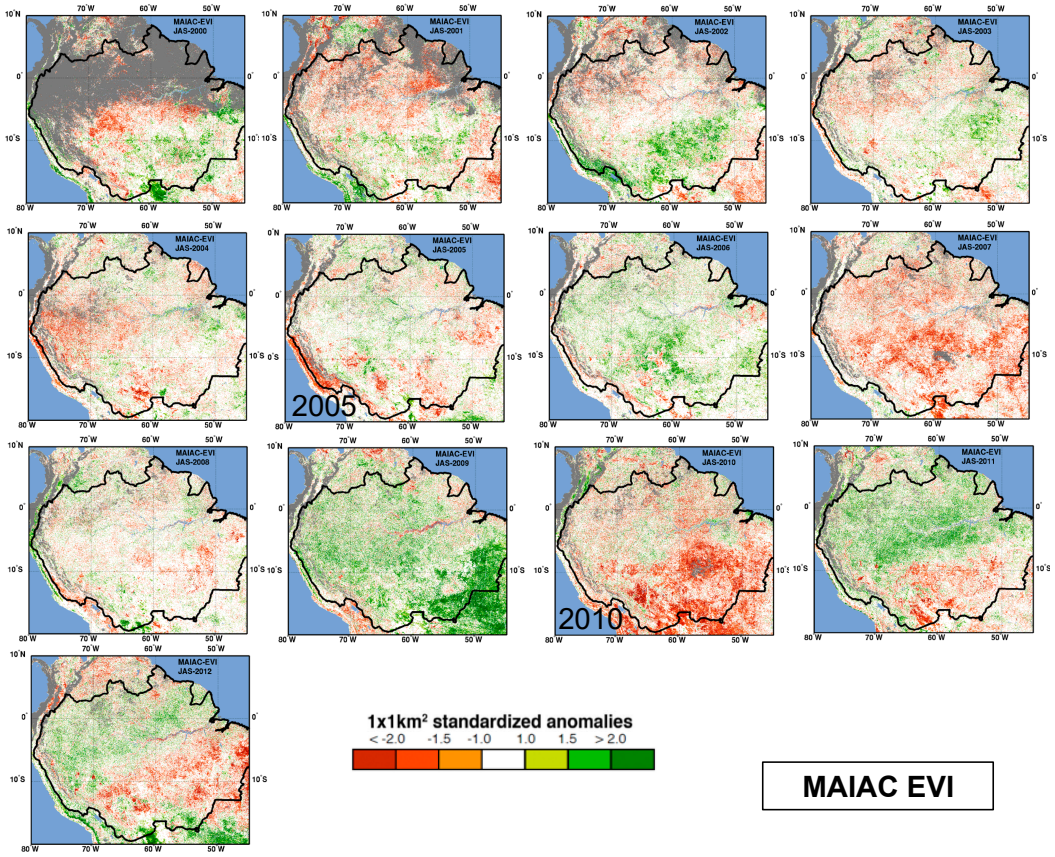

Figure S7. Spatial patterns of standardized anomalies of dry-season MAIAC EVI over Amazon in the years from 2000 to 2012. Gray shaded areas are areas with missing data.

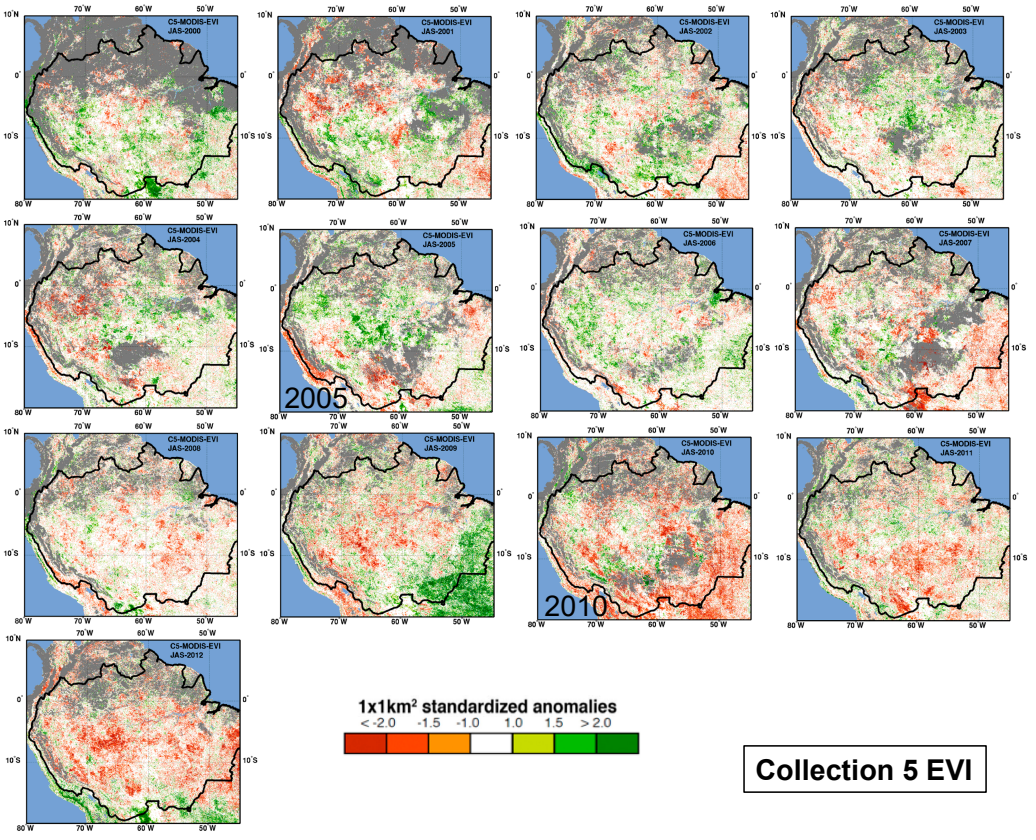

Figure S8. Spatial patterns of standardized anomalies of dry-season Collection 5 EVI over Amazon in the years from 2000 to 2012. Gray shaded areas are areas with missing data.

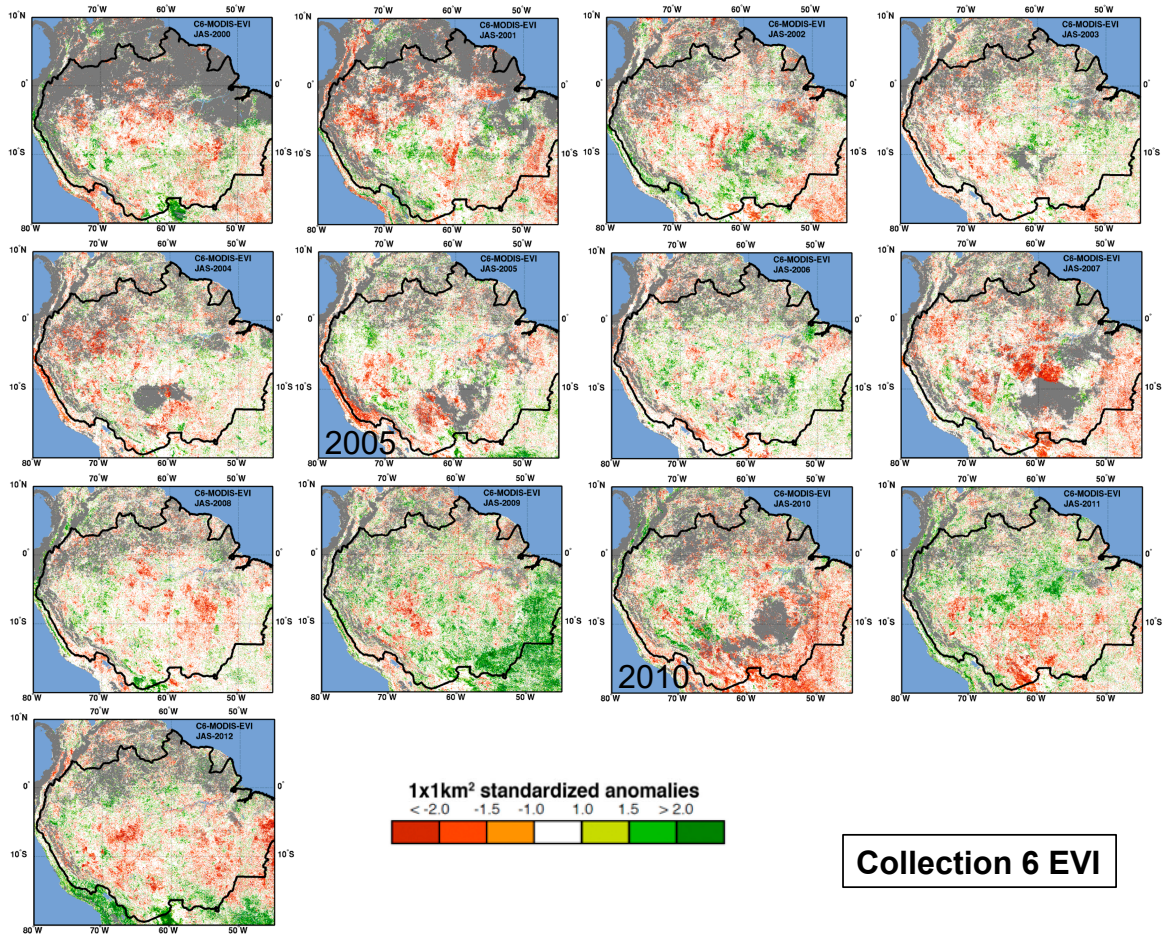

Figure S9. Spatial patterns of standardized anomalies of dry-season Collection 6 EVI over Amazon in the years from 2000 to 2012. Gray shaded areas are areas with missing data.

References

1. Friedl, M.A.; Sulla-Menashe, D.; Tan, B.; Schneider, A.; Ramankutty, N.; Sibley, A.; Huang, X. MODIS Collection 5 global land cover: Algorithm refinements and characterization of new datasets. *Remote Sens. Environ.* **2010**, *114*, 168–182.
2. Huffman, G.J.; Adler, R.F.; Rudolf, B.; Schneider, U.; Keehn, P.R. Global precipitation estimates based on a technique for combining satellite-based estimates, rain gauge analysis, and NWP model precipitation information. *J. Clim.* **1995**, *8*, 1284–1295.
3. Huete, A.; Didan, K.; Miura, T.; Rodriguez, E.P.; Gao, X.; Ferreira, L.G. Overview of the radiometric and biophysical performance of the MODIS vegetation indices. *Remote Sens. Environ.* **2002**, *83*, 195–213.
4. Lyapustin, A.I.; Wang, Y.; Laszlo, I.; Hilker, T.; G Hall, F.; Sellers, P.J.; Tucker, C.J.; Korkin, S.V. Multi-angle implementation of atmospheric correction for MODIS (MAIAC): 3. Atmospheric correction. *Remote Sens. Environ.* **2012**, *127*, 385–393.
5. Lyapustin, A.; Martonchik, J.; Wang, Y.; Laszlo, I.; Korkin, S. Multiangle implementation of atmospheric correction (MAIAC): 1. Radiative transfer basis and look-up tables. *J. Geophys. Res. Atmos.* **2011**, *116*, doi:10.1029/2010jd014985.
6. Lyapustin, A.; Wang, Y.; Frey, R. An automatic cloud mask algorithm based on time series of MODIS measurements. *J. Geophys. Res. Atmos.* **2008**, *113*, doi:10.1029/2007jd009641.
7. Lyapustin, A.; Wang, Y.; Laszlo, I.; Kahn, R.; Korkin, S.; Remer, L.; Levy, R.; Reid, J. Multiangle implementation of atmospheric correction (MAIAC): 2. Aerosol algorithm. *J. Geophys. Res. Atmos.* **2011**, *116*, doi:10.1029/2010jd014986.
8. Hilker, T.; Lyapustin, A.I.; Tucker, C.J.; Sellers, P.J.; Hall, F.G.; Wang, Y. Remote sensing of tropical ecosystems: Atmospheric correction and cloud masking matter. *Remote Sens. Environ.* **2012**, *127*, 370–384.

9. Samanta, A.; Ganguly, S.; Hashimoto, H.; Devadiga, S.; Vermote, E.; Knyazikhin, Y.; Nemani, R.R.; Myneni, R.B. Amazon forests did not green-up during the 2005 drought. *Geophys. Res. Lett.* **2010**, *37*, doi:10.1029/2009gl042154.
10. Xu, L.; Samanta, A.; Costa, M.H.; Ganguly, S.; Nemani, R.R.; Myneni, R.B. Widespread decline in greenness of Amazonian vegetation due to the 2010 drought. *Geophys. Res. Lett.* **2011**, *38*, doi:10.1029/2011gl046824.